Mononuclear Phagocyte System Depletion Blocks Interstitial Tonicity-Responsive Enhancer Binding Protein/Vascular Endothelial Growth Factor C Expression and Induces Salt-Sensitive Hypertension in Rats

Agnes Machnik, Anke Dahlmann, Christoph Kopp, Jennifer Goss, Hubertus Wagner, Nico van Rooijen, Kai-Uwe Eckardt, Dominik N. Müller, Joon-Keun Park, Friedrich C. Luft, Dontscho Kerjaschki and Jens Titze

Hypertension 2010, 55:755-761: originally published online February 8, 2010
doi: 10.1161/HYPERTENSIONAHA.109.143339
Hypertension is published by the American Heart Association. 7272 Greenville Avenue, Dallas, TX 72514
 Print ISSN: 0194-911X. Online ISSN: 1524-4563

Mononuclear Phagocyte System Depletion Blocks Interstitial Tonicity-Responsive Enhancer Binding Protein/Vascular Endothelial Growth Factor C Expression and Induces Salt-Sensitive Hypertension in Rats

Agnes Machnik, Anke Dahlmann, Christoph Kopp, Jennifer Goss, Hubertus Wagner, Nico van Rooijen, Kai-Uwe Eckardt, Dominik N. Müller, Joon-Keun Park, Friedrich C. Luft, Dontscho Kerjaschki, Jens Titze

Abstract—We showed recently that mononuclear phagocyte system (MPS) cells provide a buffering mechanism for salt-sensitive hypertension by driving interstitial lymphangiogenesis, modulating interstitial Na^+ clearance, and increasing endothelial NO synthase protein expression in response to very high dietary salt via a tonicity-responsive enhancer binding protein/vascular endothelial growth factor C regulatory mechanism. We now tested whether isotonic saline and deoxycorticosterone acetate (DOCA)-salt treatment leads to a similar regulatory response in Sprague-Dawley rats. Male rats were fed a low-salt diet and received tap water (low-salt diet LSD), 1.0% saline (high-salt diet HSD), or DOCA+1.0% saline (DOCA-HSD). To test the regulatory role of interstitial MPS cells, we further depleted MPS cells with clodronate liposomes. HSD and DOCA-HSD led to Na^+ accumulation in the skin, MPS-driven tonicity-responsive enhancer binding protein/vascular endothelial growth factor C–mediated hyperplasia of interstitial lymph capillaries, and increased endothelial NO synthase protein expression in skin interstitium. Clodronate liposome MPS cell depletion blocked MPS infiltration in the skin interstitium, resulting in unchanged tonicity-responsive enhance binding protein/vascular endothelial growth factor C levels and absent hyperplasia of the lymph capillary network. Moreover, no increased skin endothelial NO synthase protein expression occurred in either clodronate liposome–treated HSD or DOCA-salt rats. Thus, absence of the MPS-cell regulatory response converted a salt-resistant blood-pressure state to a salt-sensitive state in HSD rats. Furthermore, salt-sensitive hypertension in DOCA-salt rats was aggravated. We conclude that MPS cells act as onsite controllers of interstitial volume and blood pressure homeostasis, providing a local regulatory salt-sensitive tonicity-responsive enhancer binding protein/vascular endothelial growth factor C–mediated mechanism in the skin to maintain normal blood pressure in states of interstitial Na^+ and Cl^- accumulation. Failure of this physiological extrarenal regulatory mechanism leads to a salt-sensitive blood pressure response. **(*Hypertension*. 2010;55:755-761.)**

Key Words: salt sensitivity ■ DOCA-salt ■ lymphangiogenesis ■ skin ■ Na^+ storage ■ extracellular volume

Traditionally, researchers focus on the kidney, the brain, the heart, the adrenal gland, or the blood vessels to explain the pathogenesis of hypertension.[1] A recent dietary intervention study suggested that refractory hypertension is eminently salt sensitive.[2] Salt-sensitive hypertension is commonly believed to be a "renal affair." The prevailing view on the causal relationship among salt intake, total body Na^+ and fluid balance, and blood pressure (BP) follows the basic notion that extracellular bodily fluids are in equilibrium,[3–5] that the kidney controls total body Na^+ content and thereby the extracellular volume exclusively, and that increases in extracellular volume lead to increased BP.[6,7] The underlying concept of extracellular Na^+, volume, and BP homeostasis controlled by the kidney relies on the idea that interstitial Na^+ is readily equilibrated with plasma Na^+, can be easily mobilized into the bloodstream, and that the kidneys control interstitial Na^+ and volume indirectly by means of blood purification.

In earlier studies, we questioned the widely accepted view that extracellular fluids are in equilibrium. We found instead

Received September 18, 2009; first decision October 7, 2009; revision accepted January 11, 2010.

From the Department of Nephrology and Hypertension and Nikolaus-Fiebiger Center for Molecular Medicine (A.M., A.D., C.K., J.G., K.-U.E., J.T.), Friedrich-Alexander University, Erlangen-Nürnberg, Germany; Max Rubner-Institute (H.W.), Federal Research Institute of Nutrition and Food, Kulmbach, Germany; Department of Molecular Cell Biology (N.v.R.), Vrije University Amsterdam, Amsterdam, The Netherlands; Experimental and Clinical Research Center (D.N.M., F.C.L.), Medical Faculty of the Charité, Max-Delbrück Center for Molecular Medicine, HELIOS Klinikum Berlin-Brandenburg, Berlin, Germany; Division of Nephrology (J.-K.P.), Department of Medicine, Hannover Medical School, Hannover, Germany; Department of Pathology (D.K.), Medical University Vienna, Vienna, Austria.

Correspondence to Jens Titze, Nikolaus-Fiebiger Center for Molecular Medicine, Glückstr 6, 91054 Erlangen, Germany. E-mail jtitze@molmed.uni-erlangen.de

Hypertension **is available at http://hyper.ahajournals.org** **DOI: 10.1161/HYPERTENSIONAHA.109.143339**

that Na^+ is stored in the skin, with higher concentrations compared to blood, in animals fed a high-salt diet (HSD).[8–11] Recently, we showed that interstitial mononuclear phagocyte system (MPS) cells act as such extrarenal regulators of interstitial Na^+ and water homeostasis.[12] We experimentally induced hypertonic Na^+ storage in the skin and interstitial MPS infiltration. In response to Na^+-mediated osmotic stress, MPS cells activated tonicity-responsive enhancer binding protein (TonEBP), which binds to the vascular endothelial growth factor (VEGF) C (VEGF-C) gene. By commanding VEGF-C expression, the MPS response to osmotic stress via TonEBP results in increased density and hyperplasia of the lymph-capillary network in the interstitium and in increased protein expression of endothelial NO synthase (eNOS) in interstitial cells.

In our earlier study, we induced hypertonic Na^+ accumulation, which activates the TonEBP/VEGF-C–driven regulatory cascade in MPS cells by subjecting rats to an 8% salt diet plus 0.9% sodium chloride in drinking water. Other than the compensatory MPS-driven changes in lymph capillary structure and eNOS expression, such massive dietary salt loading led to salt-sensitive hypertension in Sprague-Dawley rats. Additional experimental depletion of the MPS cells or blockade of VEGF-C with its receptors VEGF receptor 3 and/or VEGF receptor 2 blocked the regulatory response of MPS cells to interstitial Na^+ accumulation and augmented salt-sensitive hypertension, suggesting that MPS cells provide a buffering mechanism for hypertension.[12]

Here we asked whether our initial findings were restricted to an experimental approach with massive dietary salt loading only or whether more moderate dietary salt loading with 1.0% saline in drinking water, a challenge that does not usually increase BP in Sprague-Dawley rats, leads to MPS infiltration and activation of the TonEBP/VEGF-C regulatory axis in the skin. Furthermore, we speculated that blockade of this compensatory interstitial MPS response might convert the rats from a salt-resistant to a salt-sensitive state. Finally, this study represents the first test of role of MPS on volume and BP homeostasis in rats with deoxycorticosterone actetate (DOCA) treatment and 1.0% saline in drinking water. In earlier studies, we had shown that this model features salt-sensitive hypertension associated with Na^+ storage in the skin.[9,13,14]

Methods

Animal Experiments

Local government authorities approved the studies and the experiments, according to internationally accepted criteria. We randomly assigned male Sprague-Dawley rats aged 8 to 9 weeks to 6 groups: groups 1 and 2 were assigned to a low-salt diet (LSD; <0.1% NaCl) and tap water. Groups 3 through 6 were also fed a low-salt chow (<0.1% NaCl) but received salt loading by 1.0% saline water to drink (HSD). Groups 5 and 6 were additionally treated with 100-mg DOCA acetate pellets SC (DOCA-HSD). To assess the role of MPS cells in the control of volume and BP homeostasis, groups 2, 4, and 6 received clodronate liposomes (Clod) IP every 72 hours for MPS depletion.[12,15] Two days before the end of the experiment, we placed the rats in a metabolic cage and sampled urine for 24 hours. At the end of both rat experiments after 2 weeks on their specified diets, we anesthetized the rats with 1.5% to 2.0% isoflurane anesthesia and catheterized the right femoral artery. We connected arterial lines to MLT0380/A transducers and a PowerLab 8/30 data acquisition system (ADInstruments) and measured arterial BP in conscious animals kept in a restrainer 2 hours after the operation; thereafter, blood samples were taken, the animals were killed, and skin and ear samples were taken for histology and assessment of protein and gene expression. We analyzed arterial blood gases with a clinical blood gas analyzer (Radiometer Copenhagen), including Na^+, K^+, and Cl^- measurements by ion-selective electrodes. Chemical analysis of the carcasses included Na^+, K^+, Cl^-, and water measurements after dry ashing of the different tissues as reported previously.[8,10] We calculated the Cl^- space as a measure of the extracellular volume from the tissue Cl^- content and the serum Cl^- concentration. The Cl^--free water space was calculated as a measure of the intracellular volume. Detailed information on the ashing protocol is provided in the online Data Supplement (please see http://hyper.ahajournals.org).

Immunohistochemistry and Immunofluorescence Staining of MPS Cells and Lymphcapillaries

We performed all of the staining using the Avidin/Biotin Blocking kit (Vector Laboratories) and horseradish peroxidase super staining kit (ID Laboratories) according to the manufacturer's instructions (please see the online Data Supplement). After staining with specific antibodies, lymph capillaries (anti-podoplanin antibody, from D. K.), MPS cells (anti-CD68 antibody, MCA1029, AbD Serotec), and VEGF-C–positive cells (anti–VEGF-C, ab9546, Abcam) were counted throughout the whole diameter of a crosswise cut rat ear. We counted lymphcapillaries in 5 consecutive sections and MPS and VEGF-C–positive cells in 6 consecutive sections and normalized capillary and cell counts per field.

Immunofluorescence of Endothelial NO Synthase Expression

We performed indirect immunofluorescence for expression of endothelial NO synthase (eNOS) in the ear with a rabbit polyclonal anti-eNOS antibody (PA1–037, Affinity BioReagents), as reported previously.[12] We analyzed specimens using a Zeiss Axioplan-2 imaging microscope with the digital image processing program AxioVision 4.3 (Zeiss).

TonEBP, VEGF-C, and Tumor Necrosis Factor-α Gene and Protein Expression

We quantified mRNA expression in skin samples by real-time PCR, as reported previously (please see the online Data Supplement for details on primer sequences).[12] VEGF-C protein expression in skin samples was quantified by Western blot analysis (VEGF-C–specific antibody, ab9546, Abcam). Serum tumor necrosis factor (TNF)-α levels were measured by ELISA, according to the manufacturer's instructions (Abcam).

Statistical Analysis

Comparison of means of data from animal experiments was calculated by multivariate or univariate analysis using the generalized linear measurements procedure. We tested for the effect of diet, DOCA treatment, and Clod treatment. All of the data in the article are presented as average±SD. Statistical analysis was performed with the SPSS software (version 17.0).

Results

Experimental MPS Depletion Induces Salt Sensitivity in Rats

BP in the rats did not increase with HSD (Figure 1A). However, BP increased when HSD rats were given Clod; the BP increase was composed of ≈10 mm Hg. In LSD rats, Clod did not increase BP. These findings suggest that MPS depletion with Clod indeed blocked a compensatory mechanism to maintain basal BP in HSD-treated rats. DOCA-HSD rats developed salt-sensitive hypertension that was paralleled

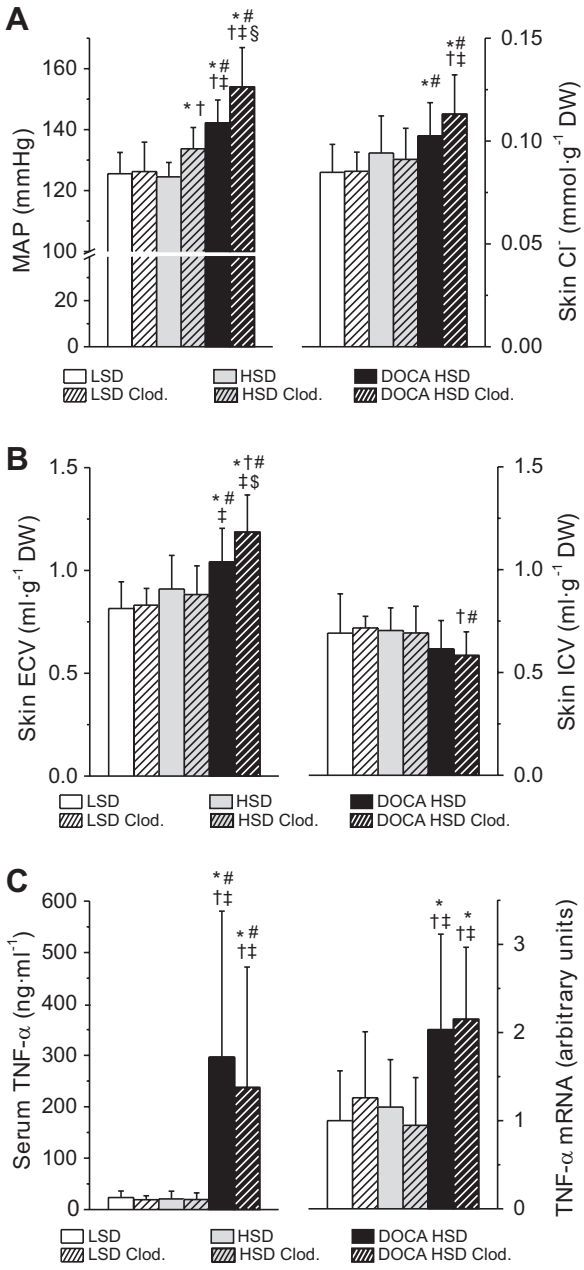

Figure 1. A, Mean arterial blood pressure (MAP) and Cl^- content in skin at the end of the study in rats with LSD diet (<0.1% NaCl chow and tap water) or HSD diet (<0.1% NaCl chow and 1.0% saline water), with or without Clod and/or DOCA treatment for 2 weeks. Clodronate treatment induced salt-sensitivity in untreated rats and deteriorated hypertension in DOCA-salt rats. B, Chloride space and chloride-free space measurements as estimates for extracellular volume (ECV) and intracellular volume (ICV) in the skin. DOCA HSD increased ECV in the rats, and additional Clod treatment increased ECV further in DOCA HSD rats, but not with HSD alone. C, Serum TNF-α level and TNF-α gene expression in the skin. DOCA HSD treatment, but not HSD alone, increased both TNF-α protein and gene expression in parallel with salt-sensitive hypertension. *P<0.05 vs LSD; #P<0.05 vs LSD Clod; †P<0.05 vs HSD; ‡P<0.05 vs HSD Clod; §P<0.05 vs DOCA HSD; $$P_{(DOCA*Clod)}$<0.05.

by increased skin Cl^- content and extracellular volume (ECV) retention in the skin (Figure 1A and 1B). Adding Clod increased BP and Cl^- and extracellular volume retention in the skin further. These findings suggest that salt-sensitive hypertension in DOCA-HSD rats was paralleled by electrolyte and volume retention in the rats and that MPS depletion with Clod further augmented hypertension and volume retention in the skin.

Other than the dramatic changes in body electrolyte and water composition, DOCA treatment is known to induce an inflammatory state. Accordingly, DOCA-HSD and DOCA-HSD-plus-Clod–treated rats exhibited less weight gain (Table) and showed tissue Na^+ retention, water retention, and tissue K^+ loss (Table), as well as hypokalemia, metabolic alkalosis (Table), increased serum TNF-α levels, and increased TNF-α mRNA expression in the skin (Figure 1C). This inflammatory response was paralleled by proteinuria in the DOCA-HSD rats, which was aggravated by Clod. In contrast to DOCA-HSD hypertension, the de novo salt sensitivity induced in HSD rats by Clod treatment was paralleled solely by a modest increase in urinary protein excretion (Table) and no increase in TNF-α expression.

Salt Loading Induces MPS/TonEBP/VEGF-C–Driven Lymphocapillary Network Hyperplasia and Increases eNOS Expression

HSD and DOCA-HSD increased interstitial MPS and VEGF-C–positive cells in the cutaneous interstitium of the rat ear (Figure 2A and Figure S2 in the online Data Supplement, please see http://hyper.ahajournals.org). The MPS accumulation with HSD and with DOCA-HSD was accompanied by slight Na^+ accumulation without a detectable increase in water content in the skin in HSD rats and by pronounced Na^+ and water retention in the skin in DOCA-HSD rats (Table). Skin Na^+ accumulation in rats with HSD alone and in DOCA-HSD rats led to an increased Na^+:water ratio in the skin (Table) and was paralleled by increased mRNA expression of TonEBP in the skin (Figure 2B), where the $(Na^+ + K^+)$:water ratio was significantly higher than in plasma (Table). This state of affairs suggests that osmotic stress is a critical feature in this cutaneous interstitium microenvironment accumulating salt. TonEBP induces VEGF-C expression. Consequently, both HSD and DOCA-HSD increased VEGF-C mRNA (Figure 2B) and the VEGF-C protein expression in the skin (Figure 3). Activation of the TonEBP/VEGF-C regulatory axis was paralleled by increased podoplanin mRNA expression, which is a marker protein of lymph endothelial cells (Figure 2B), and was associated with hyperplasia of the lymph-capillary network in HSD and DOCA-HSD rats (Figure 2A and Figure S3), featuring increased interstitial lymph capillary count in rat ear samples. Furthermore, increased TonEBP/VEGF-C levels were paralleled by increased eNOS protein expression in the skin (Figure 4A), which did not colocalize with the lymph capillary network (Figure 4B), indicating that the lymph endothelium was not a source of increased capillary eNOS expression, suggesting that increased eNOS protein expression with HSD or DOCA-HSD originated from blood capillary endothelial cells.

Experimental MPS Depletion Prevents the Interstitial Compensatory Response to Dietary Salt

Clod effectively depleted MPS cells into the cutaneous interstitium (Figure 2A and Figure S2). In both HSD rats and

Table. Body and Tissue Electrolyte and Water Analysis, Blood Gas Analysis, and Urinary Protein Excretion

Parameter	LSD	LSD and Clod	HSD	HSD and Clod	DOCA-HSD	DOCA-HSD and Clod
Body and tissue weights						
BW start, g	278.0±13.2	272.6±19.6	277.9±16.9	278.2±13.5	276.3±9.6	277.3±13.9
BW end, g	359.3±22.2	342.2±21.8	361.0±20.2	355.6±20.4	342.1±23.6	343.4±26.9
ΔBW, g	81.4±15.6	69.6±4.7	83.1±14.2†	77.5±15.5	65.8±18.3‡	66.1±1.9‡
WW, g	305.0±21.0	286.7±22.0	300.5±16.5	298.5±20.1	281.7±23.3*‡	284.0±24.4
DW, g	101.0±8.1	94.2±8.9	97.2±8.2	97.6±6.3	88.4±8.6*‡§	87.2±9.5*‡§
Skin WW, g	62.9±7.8	58.5±5.9	61.2±4.4	61.4±5.2	54.5±5.0*‡§	56.1±6.6*‡§
Skin DW, g	25.2±3.1	23.0±2.5	23.5±2.6	23.9±1.8	20.6±2.2*‡§	20.3±2.9*‡§
Body and tissue electrolyte and water content						
Total body Na^+, mmol/g DW	0.157±0.013	0.162±0.005	0.166±0.011	0.163±0.010	0.199±0.009*†‡§	0.205±0.013*†‡§
Total body K^+, mmol/g DW	0.202±0.013	0.200±0.015	0.211±0.014	0.208±0.015	0.186±0.007*†‡§	0.187±0.010*‡§
Total body water, mL/g DW	2.023±0.111	2.049±0.073	2.099±0.120	2.061±0.101	2.192±0.068*†‡§	2.267±0.107*†‡§
Skin Na^+, mmol/g DW	0.154±0.018	0.162±0.011	0.177±0.018*	0.171±0.014*	0.193±0.016*†‡§	0.209±0.024*†‡§¶
Skin K^+, mmol/g DW	0.104±0.007	0.106±0.007	0.107±0.006	0.104±0.009	0.097±0.009‡	0.096±0.008*†‡
Skin water, mL/g DW	1.506±0.189	1.548±0.057	1.614±0.119	1.575±0.116	1.653±0.088*†	1.770±0.129*†‡§‖¶
Skin Na^+/skin water, mmol/mL	0.103±0.005	0.105±0.003	0.109±0.004*†	0.108±0.004*	0.117±0.010*†‡§	0.118±0.005*†‡§
Skin, $Na^+ + K^+$/skin water, mmol/mL	0.172±0.010	0.173±0.004	0.176±0.004	0.174±0.007	0.176±0.011	0.172±0.004
Blood gas analysis, plasma electrolytes, and urinary protein excretion						
pH	7.47±0.04	7.48±0.02	7.47±0.02	7.47±0.02	7.55±0.02*†‡§	7.55±0.02*†‡§
Po_2, mm Hg	87.0±7.6	85.4±11.1	86.1±4.5	84.8±6.6	80.8±8.3	79.8±6.5*‡
Pco_2, mm Hg	37.7±4.0	38.2±2.9	37.6±2.1	38.1±2.5	42.4±3.0*†‡§	41.1±2.8*‡§
Plasma Na^+, mmol/L	139.2±1.2	139.4±1.3	140.0±1.8	140.1±1.3	142.2±1.7*†‡§	141.4±1.9*†
Plasma K^+, mmol/L	4.28±0.32	4.21±0.36	4.18±0.36	4.17±0.37	2.25±0.25*†‡§	2.29±0.18*†‡§
Plasma Cl^-, mmol/L	104.1±0.7	102.5±2.2	103.4±2.6	103.1±0.6	95.3±1.6*†‡§	94.3±1.7*†‡§
Plasma HCO_3^-, mmol/L	27.6±0.5	28.3±0.9	27.6±1.1	27.9±0.8	36.2±1.4*†‡§	36.0±1.6*†‡§
Anion gap, mmol/L	7.9±1.3	8.9±1.7	9.6±1.6*	9.5±1.2*	10.2±1.5*	10.8±0.8*†‡§
Urinary protein, mg/d	18.2±5.1	16.1±4.7	22.5±4.3*†	23.5±7.3†	47.3±20.1*†‡§	199.7±164.6*†‡§‖¶

In the body and tissue weights section, data show the in vivo body weight (BW) at the begin and end of the study, total carcass body weight (WW) and dry weight (DW) at the end of the study, skin wet (SKWW), and dry weight (SKDW) at the end of the study in rats with LSD diet (<0.1% NaCl chow and tap water) or HSD diet (<0.1% NaCl chow and 1.0% saline water), with or without Clod and DOCA treatment for 2 weeks. DOCA-salt treatment reduced body and skin DW, indicating growth retardation, whereas HSD and HSD Clod had no effect on body weight. In the body and tissue electrolyte and water content section, data show the total body and skin electrolyte and water content in the rats. HSD alone and HSD Clod did not increase electrolyte and water contents in the rats. DOCA treatment increased Na^+ and water content in the body and in the skin. Na^+ and water contents were highest in DOCA HSD rats with additional Clod. In the blood gas analysis, plasma electrolytes, and urinary protein excretion section, both DOCA HSD and DOCA HSD Clod led to hypochloremic and hypokalemic metabolic alkalosis, whereas HSD and HSD Clod did not. HSD slightly increased urinary protein excretion, and DOCA HSD increased proteinuria further. Additional Clod treatment exacerbated proteinuria in DOCA HSD rats but not in rats with HSD alone.

*$P<0.05$ vs LSD.
†$P<0.05$ vs LSD Clod.
‡$P<0.05$ vs HSD.
§$P<0.05$ vs HSD Clod.
‖$P<0.05$ vs DOCA HSD.
¶$P_{(DOCA*Clod)}<0.05$.

DOCA-HSD rats, experimental MPS depletion with Clod blocked infiltration of VEGF-C–positive MPS cells into the cutaneous interstitium (Figure 2A). In parallel, MPS depletion in HSD and DOCA-HSD rats reduced TonEBP and VEGF-C mRNA expression (Figure 2B), as well as VEGF-C protein expression (Figure 3) in the skin, to control levels. In the absence of the TonEBP/VEGF-C response in HSD and DOCA-HSD rats with MPS depletion, the rats no longer showed hyperplasia of the lymph capillary network in the skin (Figure 2A and Figure S3), and eNOS protein expression was reduced to the control level (Figure 4). In DOCA-HSD rats, absence of hyperplasia of the lymphocapillary network was paralleled by further interstitial Cl^- (Figure 1A) and volume retention (Figure 1B), as well as further BP increase. These findings suggest that MPS cells are required to maintain BP at low levels in states of NaCl accumulation. MPS cells either induce hyperplasia of the lymph capillary network, which facilitates mobilization of interstitial volume, or increase eNOS protein expression in response to isotonic dietary salt loading and provide a

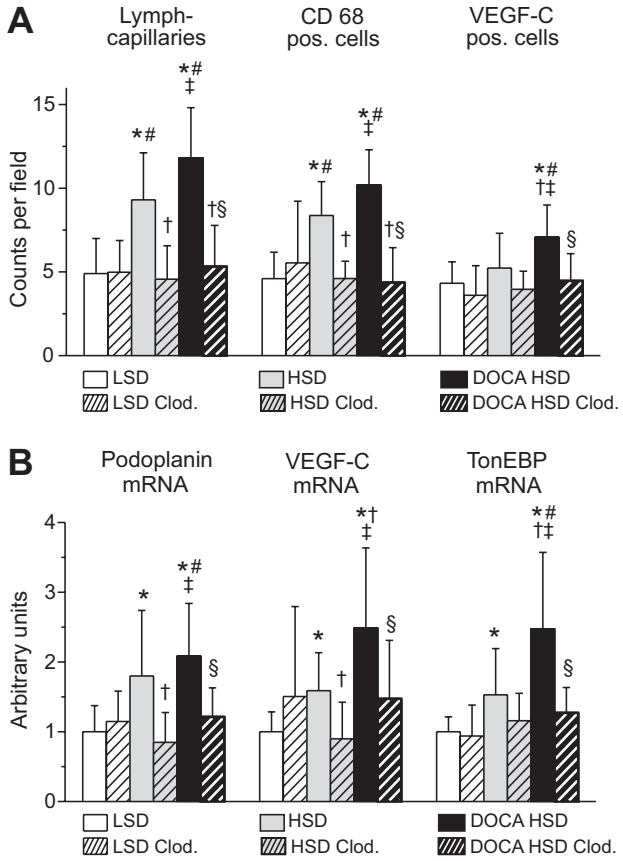

Figure 2. A, Changes in lymph capillary count, MPS cell count, and VEGF-C pos. cell count in ear. B, Changes in gene expression of podoplanin, VEGF-C, and TonEBP in the abdominal skin in the same rats. HSD and DOCA HSD increased both the number of VEGF-C positive MPS cells in ear and VEGF-C gene expression in the skin. MPS depletion with Clod left VEGF-C positive MPS cell count, as well as VEGF-C and TonEBP gene expression at the control level, despite accumulation of hypertonic saline in the skin. *$P<0.05$ vs LSD; #$P<0.05$ vs LSD Clod; †$P<0.05$ vs HSD; ‡$P<0.05$ vs HSD Clod, §$P<0.05$ vs DOCA HSD.

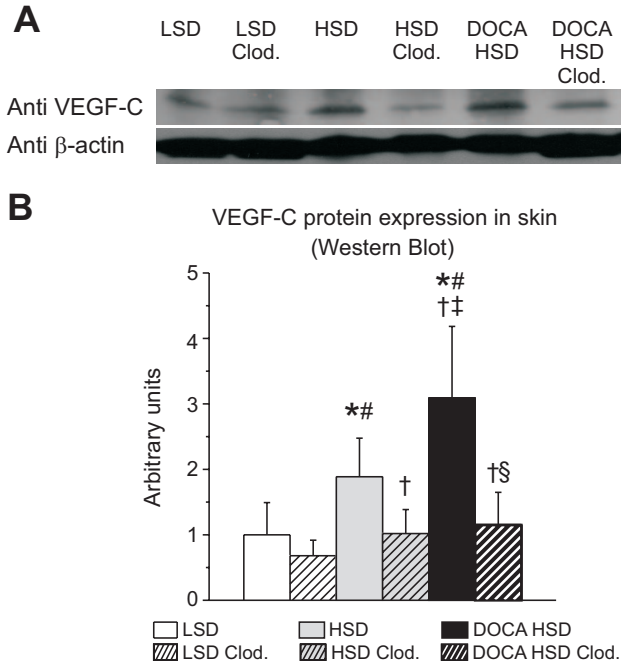

Figure 3. A, Representative Western blot of VEGF-C protein expression (47 kD) compared with β-actin expression (42 kD) in skin of rats given tap water (LSD) or 1.0% saline (HSD), with or without additional MPS cell depletion by Clod treatment, with or without additional DOCA treatment. HSD treatment increased skin VEGF-C protein expression, and DOCA HSD increased VEGF-C protein expression in the skin even further. Additional Clod treatment reversed this effect back to the control level in both HSD- and DOCA HSD–treated rats. B, Statistical analysis of VEGF-C protein expression in skin. *$P<0.05$ vs LSD; #$P<0.05$ vs LSD Clod, †$P<0.05$ vs HSD; ‡$P<0.05$ vs HSD Clod, §$P<0.05$ vs DOCA HSD.

buffering mechanism for hypertension via a TonEBP/VEGF-C regulatory axis.

Discussion

The important finding in our study is that we demonstrate conversion from a salt-resistant BP state to a salt-sensitive BP state by depleting MPS cells from the body with Clod. Clod with LSD had no influence on BP. We also found that the DOCA-HSD model (without uninephrectomy) was made even more salt sensitive by depleting MPS cells. Our new findings in animals given oral 1% saline support the physiological relevance of our recent contention that MPS cells act as regulators of volume and BP homeostasis via a TonEBP/VEGF-C regulatory mechanism. We contend that this mechanism buffers the development of salt-sensitive hypertension, either by increased lymph capillary transport capacity of interstitial fluid or by compensatory increases in eNOS expression.

We have proposed such a regulatory mechanism previously; however, the induction of salt-sensitive hypertension and the regulatory MPS response in that study had been induced by massive hypertonic salt administration that possibly had little relevance to established models.[12] We now found that more moderate salt loading by oral 1.0% saline results in TonEBP expression, which acts as an "osmoprotective" gene in skin MPS cells.[16,17] The ratio of $(Na^+ + K^+)$:water, representing >95% of the potentially osmotically effective cations in the body, was 20% to 26% higher in skin than in plasma. The finding seems peculiar; however, we have made similar observations in other models previously.[8–11,13,14] Furthermore, an increase in the skin Na^+:water ratio occurred without any changes in plasma electrolyte concentrations in rats given 1% saline to drink. This finding indicates that the skin interstitium, in which MPS cells reside, represents a separate tissue-specific, extracellular microenvironment that is not necessarily represented by changes in serum electrolyte concentrations. Furthermore, this state of affairs suggests that extracellular fluids in the intravascular and interstitial compartments are not invariably in equilibrium. In the absence of detectable changes in serum Na^+ and K^+ concentrations, an increased skin Na^+:water ratio was paralleled by altered gene expression of the osmoprotective transcription factor, TonEBP, in skin MPS cells. This finding indicates that skin Na^+ accumulation leads to interstitial osmotic stress that initiates a local, MPS-driven, regulatory response. Our finding that skin Na^+ accumulation creates an interstitial microenvironment where osmotic stress

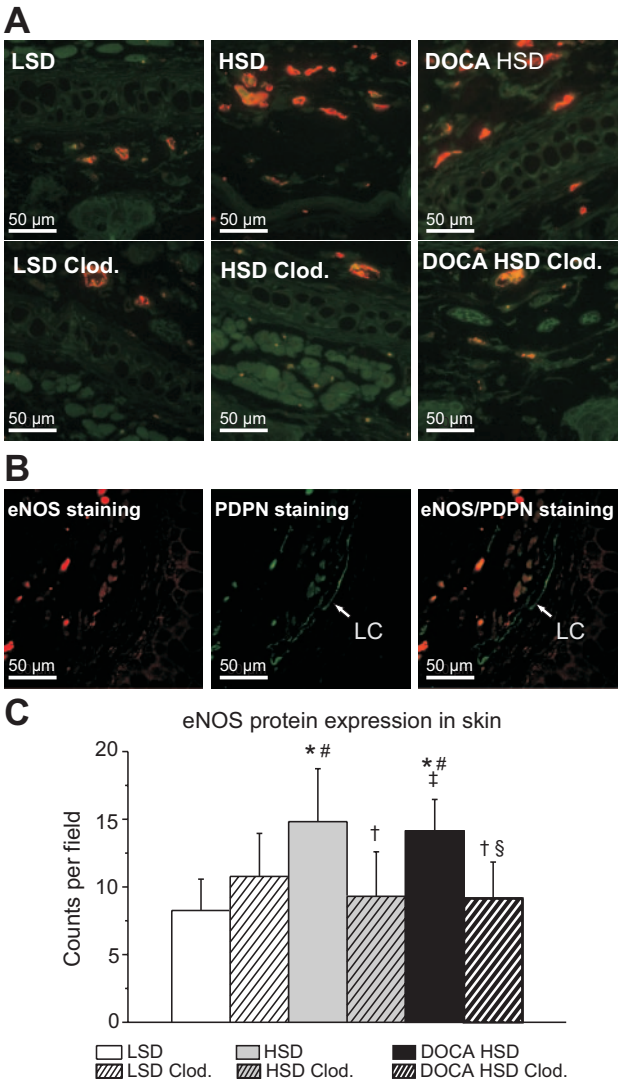

Figure 4. A, eNOS protein expression (red) in ears of rats given tap water (LSD) or 1.0% saline (HSD), with or without additional MPS cell depletion by Clod treatment, with or without additional DOCA treatment. HSD and DOCA HSD increased eNOS protein expression, and additional Clod treatment reversed this effect back to the control level. B, Colocalization of eNOS protein expression (red) and podoplanin staining (green) in the same rats. The increase of eNOS expression observed in HSD and DOCA HSD rats did not colocalize with the lymphatic endothelium of a lymph capillary (LC). C, Summary of changes in eNOS protein expression in skin (rat ear). eNOS expression in skin in response to HSD and/or DOCA HSD treatment was dependent on MPS activity. *$P<0.05$ vs LSD; #$P<0.05$ vs LSD Clod; †$P<0.05$ vs HSD; ‡$P<0.05$ vs HSD Clod, §$P<0.05$ vs DOCA HSD.

is a critical feature of MPS cell function receives support from Go et al,[18] who found that osmotic stress is a critical feature for lymphatic function. Their data suggest that immune cells residing in the interstitial space, even without dietary salt loading, confront a microenvironment that is characterized by hypertonicity compared with plasma. We are aware that we must develop accurate novel methods to measure osmolality in these compartments in vivo. However, in vitro cell-based experiments render support for our conclusion.[12,19]

We showed earlier that activation of the TonEBP/VEGF-C regulatory axis induced hyperplasia of the lymph capillary network in the skin and increased eNOS protein expression in interstitial endothelial cells.[12] We were able to corroborate those findings here. In addition, we could show that the increase in skin eNOS protein expression is not explained by increased eNOS expression in the lymph capillary network, because eNOS protein and podoplanin protein as a marker for lymph-endothelial cells did not colocalize with eNOS expression. We conclude that increased eNOS protein expression, which we have shown previously to be MPS and VEGF-C dependent,[12] does not originate from increased lymph endothelial cell mass in the lymph capillary network. This finding is important, because lymph endothelial cells have the potential to express eNOS in vitro and in vivo.[20–22]

MPS cells are diverse and develop into morphological and functional distinct cell types in response to the tissue microenvironment. Although MPS cells are uniformly found in hypertensive target-organ damage lesions, the relative contribution of the MPS cell subsets to the "inflammatory" response in atherosclerosis is complex.[23–26] Tipping the balance of macrophage polarization into more proatherogenically activated M1 subtypes or rather more antiatherogenic programs in M2 subtypes is considered to affect pathogenesis, evolution, and complications of target organ damage.[25] Our data provide preliminary evidence that MPS cells may act as regulators of volume and BP homeostasis in response to dietary salt loading without inducing a concomitant inflammatory response. The findings support the idea that MPS/TonEBP/VEGF-C activity might represent an "M2 feature" of MPS cell function. TNF-α is a typical indicator for M1-type polarization of MPS cells. In our rats, MPS cell infiltration into the skin in response to HSD induced the TonEBP/VEGF-C regulatory axis without concomitant TNF-α gene and protein expression from the MPS. Furthermore, the BP increase after nonselective MPS blockade with Clod did not increase TNF-α in HSD rats. In contrast, interstitial MPS infiltration in HSD rats with additional DOCA treatment, which induces salt-sensitive hypertension and target organ damage in the long term in the rats, was paralleled not only by increased TNF-α expression but also led to proteinuria and reproducibly leads to stunted growth with decreased tissue weights, as shown in the Table and in our previous studies in DOCA-salt rats.[9,13,14] These findings suggest that DOCA-HSD treatment induces a chronic inflammatory state. Interestingly, the TNF-α gene in DOCA-HSD rats remained highly expressed after additional nonselective MPS depletion with Clod. Moreover, proteinuria worsened with BP increase, whereas the TonEBP/VEGF-C regulatory response of the lymph capillary network and eNOS protein expression were blocked. These findings suggest that MPS cells contribute to prevent salt-induced hypertension and that interstitial MPS infiltration may be beneficial by providing a net protective effect against hypertension-induced target organ damage.

Perspectives

We suggest expanding the horizon of salt-sensitive BP research to include a third compartment: novel molecular

regulators, MPS involvement, and local lymph and blood capillary participation. We present a novel, albeit unconventional, schema featuring MPS cells that modulate BP via TonEBP/VEGF-C and a vascular bed hitherto fore largely ignored, namely, the lymphocapillary network. It remains to be investigated whether the salt-sensitive BP increase that we found by the acute method of BP measurement in restrained animals is present in chronically instrumented animals as well. Radiotelemetric BP measurements may answer this question and also may provide information on the time course of the BP increase after experimental MPS depletion. Furthermore, it is tempting to speculate that animals with VEGF-C overexpression are protected from developing hypertension. Vice versa, it may be speculated that selective VEGF receptor 3 blockade, a favorite concept in cancer therapy, may increase BP by blocking MPS regulatory activity in volume and BP homeostasis. Finally, the fact has not escaped us that human subject research is required in this area. Microdialysis techniques and magnetic resonance–based 23Na methods should be helpful and are areas that we are pursuing.

Acknowledgments

We thank Elke Prell, Birgit Hausknecht, Monika Klewer, and Esther Ermeling for their technical assistance.

Sources of Funding

This study was supported by grants from the German Research Foundation (Ti345/2) and the Federal Ministry of Economics and Technology/German Aerospace Center (BMWi/DLR; 50WB0920) to J.T. D.N.M. was supported by a Helmholtz Fellowship.

Disclosures

None.

References

1. Marvar PJ, Gordon FJ, Harrison DG. Blood pressure control: salt gets under your skin. *Nat Med*. 2009;15:487–488.
2. Pimenta E, Gaddam KK, Oparil S, Aban I, Husain S, Dell'Italia LJ, Calhoun DA. Effects of dietary sodium reduction on blood pressure in subjects with resistant hypertension: results from a randomized trial. *Hypertension*. 2009;54:475–481.
3. Pitts RF. Volume and composition of the body fluids. In: Pitts RF, ed. *Physiology of the Kidney and Body Fluids.* Chicago, IL: Year Book Medical Publishers; 1974:11–34.
4. Strauß MB, Lamdin E, Smith WP, Bleifer DJ. Surfeit and deficit of sodium: a kinetic concept of sodium excretion. *Arch Int Med*. 1958;102:527–536.
5. Bernard C. *Leçons sur les Propriétés Physiologiques et les Altérations Pathologiques des Liquides de l'Organisme.* Paris, France: Baillière; 1859.
6. Guyton AC, Coleman TG, Cowley AW Jr, Liard JF, Norman RA Jr, Manning RD Jr. Systems analysis of arterial pressure regulation and hypertension. *Ann Biomed Eng*. 1972;1:254–281.
7. Lifton RP, Gharavi AG, Geller DS. Molecular mechanisms of human hypertension. *Cell*. 2001;104:545–556.
8. Schafflhuber M, Volpi N, Dahlmann A, Hilgers KF, Maccari F, Dietsch P, Wagner H, Luft FC, Eckardt KU, Titze J. Mobilization of osmotically inactive Na+ by growth and by dietary salt restriction in rats. *Am J Physiol Renal Physiol*. 2007;292:F1490–F1500.
9. Titze J, Bauer K, Schafflhuber M, Dietsch P, Lang R, Schwind KH, Luft FC, Eckardt KU, Hilgers KF. Internal sodium balance in DOCA-salt rats: a body composition study. *Am J Physiol Renal Physiol*. 2005;289:F793–F802.
10. Titze J, Lang R, Ilies C, Schwind KH, Kirsch KA, Dietsch P, Luft FC, Hilgers KF. Osmotically inactive skin Na+ storage in rats. *Am J Physiol Renal Physiol*. 2003;285:F1108–F1117.
11. Titze J, Shakibaei M, Schafflhuber M, Schulze-Tanzil G, Porst M, Schwind KH, Dietsch P, Hilgers KF. Glycosaminoglycan polymerization may enable osmotically inactive Na+ storage in the skin. *Am J Physiol Heart Circ Physiol*. 2004;287:H203–H208.
12. Machnik A, Neuhofer W, Jantsch J, Dahlmann A, Tammela T, Machura K, Park JK, Beck FX, Muller DN, Derer W, Goss J, Ziomber A, Dietsch P, Wagner H, van Rooijen N, Kurtz A, Hilgers KF, Alitalo K, Eckardt KU, Luft FC, Kerjaschki D, Titze J. Macrophages regulate salt-dependent volume and blood pressure by a vascular endothelial growth factor-C-dependent buffering mechanism. *Nat Med*. 2009;15:545–552.
13. Ziomber A, Machnik A, Dahlmann A, Dietsch P, Beck FX, Wagner H, Hilgers KF, Luft FC, Eckardt KU, Titze J. Sodium-, potassium-, chloride-, and bicarbonate-related effects on blood pressure and electrolyte homeostasis in deoxycorticosterone acetate-treated rats. *Am J Physiol Renal Physiol*. 2008;295:F1752–F1763.
14. Titze J, Luft FC, Bauer K, Dietsch P, Lang R, Veelken R, Wagner H, Eckardt KU, Hilgers KF. Extrarenal Na+ balance, volume, and blood pressure homeostasis in intact and ovariectomized deoxycorticosterone-acetate salt rats. *Hypertension*. 2006;47:1101–1107.
15. Van Rooijen N, Sanders A. Liposome mediated depletion of macrophages: mechanism of action, preparation of liposomes and applications. *J Immunol Methods*. 1994;174:83–93.
16. Miyakawa H, Woo SK, Dahl SC, Handler JS, Kwon HM. Tonicity-responsive enhancer binding protein, a rel-like protein that stimulates transcription in response to hypertonicity. *Proc Natl Acad Sci U S A*. 1999;96:2538–2542.
17. Neuhofer W, Beck FX. Cell survial in the hostile environment of the renal medulla. *Annu Rev Physiol*. 2005;67:531–555.
18. Go WY, Liu X, Roti MA, Liu F, Ho SN. NFAT5/TonEBP mutant mice define osmotic stress as a critical feature of the lymphoid microenvironment. *Proc Natl Acad Sci U S A*. 2004;101:10673–10678.
19. Shapiro L, Dinarello CA. Osmotic regulation of cytokine synthesis in vitro. *Proc Natl Acad Sci U S A*. 1995;92:12230–12234.
20. Lahdenranta J, Hagendoorn J, Padera TP, Hoshida T, Nelson G, Kashiwagi S, Jain RK, Fukumura D. Endothelial nitric oxide synthase mediates lymphangiogenesis and lymphatic metastasis. *Cancer Res*. 2009;69:2801–2808.
21. Doboszynska T, Andronowska A, Modzelewska B. Immunohistochemical localisation of ET-1 and eNOS in lymphatic stomata of the porcine broad ligament of the uterus. *Folia Histochem Cytobiol*. 2001;39:15–22.
22. Leak LV, Cadet JL, Griffin CP, Richardson K. Nitric oxide production by lymphatic endothelial cells in vitro. *Biochem Biophys Res Commun*. 1995;217:96–105.
23. Galkina E, Ley K. Immune and inflammatory mechanisms of atherosclerosis (*). *Annu Rev Immunol*. 2009;27:165–197.
24. Hansson GK. Inflammation, atherosclerosis, and coronary artery disease. *N Engl J Med*. 2005;352:1685–1695.
25. Mantovani A, Garlanda C, Locati M. Macrophage diversity and polarization in atherosclerosis: a question of balance. *Arterioscler Thromb Vasc Biol*. 2009;29:1419–1423.
26. Yan ZQ, Hansson GK. Innate immunity, macrophage activation, and atherosclerosis. *Immunol Rev*. 2007;219:187–203.

Mononuclear phagocyte system depletion blocks interstitial TonEBP/VEGF-C expression and induces salt-sensitive hypertension in rats
Running head: MPS and salt-sensitive hypertension

Agnes Machnik[1], Anke Dahlmann[1], Christoph Kopp[1], Jennifer Goss[1], Hubertus Wagner[2], Nico van Rooijen[3], Kai-Uwe Eckardt[1], Dominik N. Müller[4], Joon-Keun Park[5], Friedrich C. Luft[4], Dontscho Kerjaschki[6], and Jens Titze[1]

[1] Department of Nephrology and Hypertension and Nikolaus-Fiebiger Center for Molecular Medicine, Friedrich-Alexander University, Erlangen-Nürnberg, Germany

[2] Max Rubner-Institute, Federal Research Institute of Nutrition and Food, Kulmbach, Germany

[3] Department of Molecular Cell Biology, VUMC, Amsterdam, The Netherlands

[4] Experimental and Clinical Research Center, Medical Faculty of the Charité, Max-Delbrück Center for Molecular Medicine, HELIOS Klinikum Berlin-Brandenburg, Berlin, Germany

[5] Division of Nephrology, Department of Medicine, Hannover Medical School, Germany

[6] Department of Pathology, Medical University Vienna, Vienna, Austria

Correspondence to:
Jens Titze, MD
Nikolaus-Fiebiger Center for Molecular Medicine
Glückstr. 6
91054 Erlangen, Germany
(e-mail: jtitze@molmed.uni-erlangen.de)
Tel. +49 9131 8539300
Fax +49 9131 8539311

Online material and methods

Animal experiments. Local government authorities (AZ 54–2531.31–5/07 and TS–3/07 Med IV / Nephro; Regierung von Mittelfranken, Ansbach; Germany) approved the studies and the experiments were done according to the guidelines of the American Physiological Society. We randomly assigned 70 male Sprague Dawley rats (Charles River, Sulzfeld, Germany) aged 8–9 weeks to 6 groups: Group 1 (n=15) and Group 2 (n= 11) to a low–salt diet (LSD; <0.1% NaCl) and tap water. Group 3 (n=12), Group 4 (n=12), Group 5 (n=10), and Group 6 (n=10) were also fed a low-salt chow (<0.1% NaCl), but received salt loading by 0.9% saline water to drink (HSD). Groups 5 and 6 were additionally treated with deoxycorticosterone acetate 100 mg pellets subcutaneously (DOCA-HSD). To assess the role of mononuclear phagocyte system (MPS) cells in the control of volume and blood pressure homeostasis, Groups 2, 4, and 6 received clodronate liposomes (Clod) i.p. every 72 h for MPS depletion.[1, 2] Two days before the end of the experiment, we placed the rats in a metabolic cage, and sampled urine for 24 h. We quantified urinary protein excretion with the Bradford assay. At the end of both rat experiments after 2 weeks on their specified diets, we anesthetized the rats with 1.5–2% isoflurane anesthesia and catheterized the right femoral artery. We connected arterial lines to MLT0380/A transducers and a PowerLab 8/30 data acquisition system (ADInstruments, Spechbach, Germany), and measured arterial blood pressure (BP) in conscious animals kept in a restrainer 2 h after the operation, thereafter, blood samples were taken and the animals were killed and skin and ear samples were taken for histology and assessment of protein and gene expression. We analyzed arterial blood gases with a clinical blood gas analyzer (Radiometer Copenhagen), including Na^+, K^+, and Cl^- measurements by ion-selective electrodes. Chemical analysis of the carcasses included Na^+, K^+, Cl^-, and water measurements after dry ashing of the different tissues as reported previously.[3, 4]

Ashing procedure. We completely skinned the carcasses, and removed a 2 g skeletal muscle specimen. We weighed the completely skinned rest carcasses and muscle specimen [wet weight (WW)], then desiccated at 90°C for 72 h [dry weight (DW)]. Because weights were unchanged with further drying, the difference between WW and DW was considered as tissue water content. We then ashed the tissues at 190° for 5 h, 300°C for 18 h, and 450° C for 24 h and sieved the bones from the carcass ashes. We further ashed the separated tissues at 600° C for 48 h and then dissolved in 5% or 10% HNO_3. We measured Na^+ and K^+ concentration by atomic adsorption spectrometry (Model 3100, Perkin Elmer, Rodgau, Germany), and. Cl^- concentration by titration with 0.1N silver nitrate (Model Titrando, German Metrohm, Filderstadt, Germany). We then calculated Cl^- space as a measure of the extracellular volume (ECV) from the tissue Cl^- content and the serum Cl^- concentration:

$$tissue\ Cl^-\ space = \frac{tissue\ Cl^-\ content\ (mmol)}{serum\ [Cl^-]\ (mmol/ml)} \qquad (1)$$

We then estimated intracellular volume (ICV) in the tissues was by the Cl^--free water space:

$$tissue\ Cl^-\ free\ space = tissue\ water\ content\ (ml) - tissue\ Cl^-\ space \qquad (2)$$

TonEBP and VEGF-C gene expression. We extracted total RNA from animal tissue with RNeasy Minicolumns (Qiagen, Hilden, Germany), homogenizing skin slices (~10–20 mg) in 500 µl of RLT buffer reagent with an Ultra-Turrax for 30 s. After homogenization, we added 950 µl of water and 16µl of proteinase K (25U/µl), and incubated the sample at 55°C for 10 min and then centrifuged at 12,000 rpm for 3 min. After addition of 1 ml of 96–100% ethanol, we transferred the solvent to the mini-columns and eluted according to the standard protocol.

Real-time PCR. First-strand cDNA was synthesized with TaqMan RT reagents (Applied Biosystems, Darmstadt, Germany), with random hexamers used as primers. We performed real-time PCR with an ABI PRISM 7000 sequence detector and SYBR green reagents (Applied Biosystems, Darmstadt, Germany) according to the manufacturer's instructions. Primers used for amplification are shown in Table S1. All samples were run in duplicate. We normalized the relative amount of the specific mRNA of interest with respect to 18S rRNA content in the sample. Dissociation curves confirmed the specificity of the PCR.

Table S1. Real time PCR primers

Primer	Sequence
Rat TNF-α	
Forward	GCCCAGACCCTCACACTC
Reverse	CCACTCCAGCTGCTCCTC
Rat TonEBP	
Forward	CCAATGGAAGTAACATCAGAGAAA
Reverse	CTGGGTTGATCCGACTGTCT
Rat VEGF-C	
Forward	TCCACCATCAAACATGCAGC
Reverse	TCAGTCGATTTGTACATGGTCGT
Ribosomal 18S Primers	
Forward	TTGATTAAGTCCCTGCCCTTTGT
Reverse	CGATCCGAGGGCCTCACTA

VEGF-C protein expression. We homogenized matrix proteins from shock-frozen skin in 500µl lysis buffer (50 mM Tris_HCl, pH 7.2, 150 mM NaCl, 1% Triton X-100, 1 mM sodium orthovanadate, 50 µg/ml sodium pyrophosphate, 100 mM sodium fluoride, 0.01% aprotinin, 4 µg/ml pepstatin A, 10 µg/ml leupeptin, and 1 mM phenylmethylsulfonyl fluoride) with an Ultra-Turrax for 30sec.

For immunoblotting, we separated equal amounts of total protein on 8% or 12% SDS-polyacrylamide gel under reducing conditions and electroblotted onto a polyvinylidene diflouride (PVDF) membrane. We blocked the blots with 5% nonfat milk in phosphate buffered saline (PBS) and 0.1% Tween 20, pH 7.5 for 1 h at room temperature and then incubated overnight at 4°C with Anti-VEGFC (Abcam, Cambrigde, UK). Equal amounts of protein were run on 8% SDS-polyacrylamid gels. After three washes in PBS with 0.1% Tween20 pH7.5, the we incubated the blots for 1 h with horseradisch peroxidase-conjugated anti-rabbit IgG (Pierce, Rockford, USA) diluted 1:2,000 in blocking solution at room temperature. We visualized antibody binding using an enhanced chemiluminescence system (Pierce, Rockford, USA). We scanned specific bands and quantified them by densitometry.

TNFα Elisa. TNFα Elisa was from Abcam (Cambridge, UK) and was performed according to manufacturer's instructions.

Immunhistochemistry and immunofluorescence staining of lymphcapillaries. We fixed animal tissues in 5% formalin and embedded in paraffin. We performed all staining using Avidin/Biotin Blocking Kit (Vector laboratories) and HRP super staining kit (ID Labs, Ontario, USA) according to manufacturer's instructions. Briefly, we deparaffinised slides and boiled two times for about 5 min at 600 W in a microwave in 0.1 M citrate buffer (pH 6.0). We cooled down the slides to room temperature and incubated in 3% H_2O_2 for 10 min. We then blocked the slides with Avidin/Biotin Blocking Kit (Vector laborities, Burlingame, USA) according to manufacturer's protocol and with SuperBlock for about 7 min. After three times washing with PBS, we incubated slides with first antibody for about 1 h, followed by incubation with the polyvalent antibody and HRP for 10 min. We washed the slides three times with PBS between every step. We detected specific staining using AEC Chromogen/Substrate (3-Amino-9-ethylcarbazole , ID Labs). Both lymph capillaries and MPS cells were counted throughout the whole diameter of a crosswise cut rat ear. We counted lymph capillaries counted at 125-fold amplification, and MPS cells at 300-fold amplification under the microscope. Starting from the same edge of the ear, we counted lymph capillaries in 5 consecutive fields, as indicated in Figure S1. Similarly, we counted

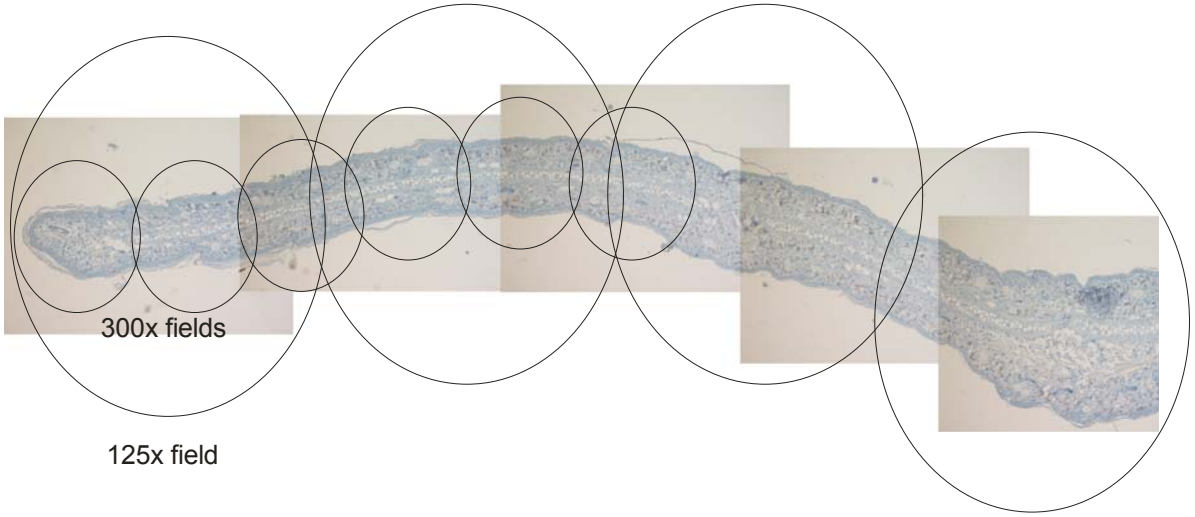

Figure S1: Scheme of sections for lymph capillary counting (125-fold field) and for MPS counting (300-fold field).

MPS cells in 6 consecutive sections and normalized capillary and MPS cell counts per field. For three-dimensional reconstruction, we fixed and stained 143 7µm-sized serial sections of ear specimens for podoplanin as described above. We performed digitalization of the serial slices using an AxioCam MRm camera (Zeiss, Germany) mounted on an Axiovert 200M microscope (Zeiss, Germany) with the fluorescence filter for Cy2 (filter set 38 HE, Zeiss). After acquisition, a stack of equal image size was built using the graphic tool ImageJ (Wayne Rasband, NIH, Bethesda, MD, USA). We imported the equalized data into the Amira 4.1 visualization software (Visage Imaging Inc., Carlsbad, California, USA) on a Dell Precision 690 computer system (Dell, Frankfurt, Germany). After this step, the podoplanin channel was aligned. In the segmentation step the podoplanin data set served as a scaffold and was spanned manually or automatically using greyscale values. Out of this segmentation matrix we

generated the volume surfaces. We reconstructed the surfaces of skin and cartilage using the fluorescence of the background-staining of the podoplanin antibody.
Antibody dilutions: Anti-Podoplanin 1:5,000 (from D. Kerjaschki), Anti-VEGFC 1:1,000 (Abcam, Cambrigde, UK).

Immunofluorescence staining of eNOS expression. Paraffin-embedded sections were dewaxed, dehydrated and antigen-demasked with 0.05% trypsin. We performed indirect immunofluorescence for expression of eNOS with a rabbit polyclonal anti-eNOS antibody (ABR, Affinity Bio reagents, CO, USA). We blocked nonspecific binding sites with 10% normal donkey serum (Jackson ImmunoResearch Laboratories, PA, USA) for 30 min in room temperature. Thereafter we incubated sections with the primary antibody for 1 h. All incubations were performed in a humid chamber at room temperature. For fluorescent visualization of bound primary antibodies, we further incubated sections with Cy3-conjugated donkey anti-rabbit antibody (Jackson ImmunoResearch Laboratories, PA, USA) for 1 h in the dark. We analyzed specimens using a Zeiss Axioplan-2 imaging microscope with the digital image-processing program AxioVision 4.3 (Zeiss, Jena, Germany). Semiquantitative analysis of eNOS expression was done by using the following scoring system: 0, absent; 1, very few; 2, few; 3, mediate; 4, much and 5, very much expression. We analyzed 10 areas per section in 5-6 rats from each group. The investigator performing these immunohistochemical analyses had no knowledge of the treatment group assignment.

Statistical analysis. Comparison of means of data from animal experiments was calculated by multivariate or univariate analysis using the General Linear Measurements (GLM) procedure. We tested for the effect of diet, clodronate treatment, and adenoviral transfer of soluble VEGFR receptor. Comparison of means in cell culture experiments was calculated by Student's T-test for paired samples. All data in the manuscript are presented as average ± SD. The term increased or decreased are used only if the results were significant at $P<0.05$. Statistical analysis was performed with the SPSS software (version 15.0).

References:

1. Machnik A, Neuhofer W, Jantsch J, Dahlmann A, Tammela T, Machura K, Park JK, Beck FX, Muller DN, Derer W, Goss J, Ziomber A, Dietsch P, Wagner H, van Rooijen N, Kurtz A, Hilgers KF, Alitalo K, Eckardt KU, Luft FC, Kerjaschki D, Titze J. Macrophages regulate salt-dependent volume and blood pressure by a vascular endothelial growth factor-C-dependent buffering mechanism. *Nat Med.* 2009;15:545-552.
2. Van Rooijen N, Sanders A. Liposome mediated depletion of macrophages: mechanism of action, preparation of liposomes and applications. *J Immunol Methods.* 1994;174:83-93.
3. Schafflhuber M, Volpi N, Dahlmann A, Hilgers KF, Maccari F, Dietsch P, Wagner H, Luft FC, Eckardt KU, Titze J. Mobilization of osmotically inactive Na+ by growth and by dietary salt restriction in rats. *Am J Physiol Renal Physiol.* 2007;292:F1490-1500.
4. Titze J, Lang R, Ilies C, Schwind KH, Kirsch KA, Dietsch P, Luft FC, Hilgers KF. Osmotically inactive skin Na+ storage in rats. *Am J Physiol Renal Physiol.* 2003;285:F1108-1117.

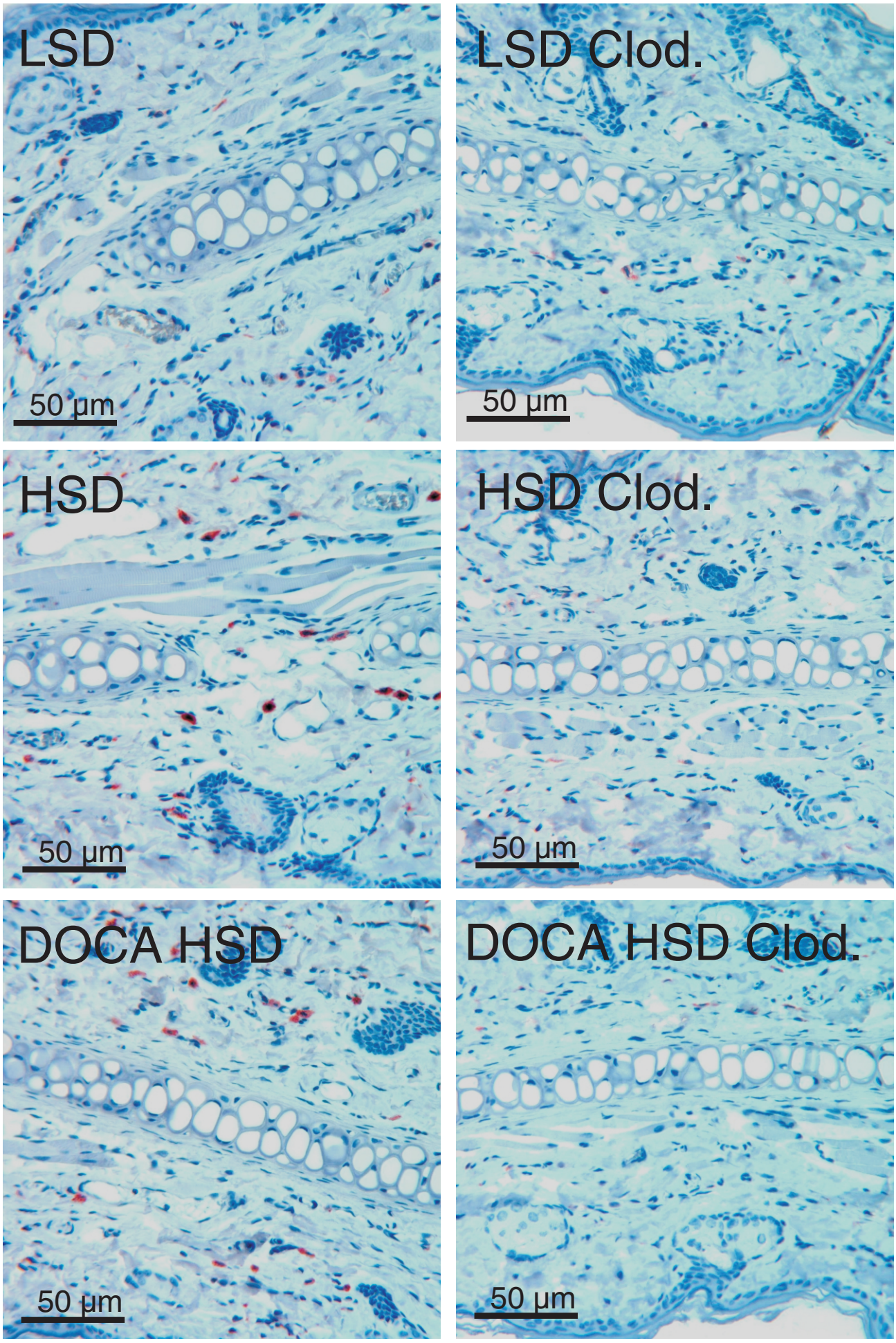

Figure S2:
MPS cells visualized with a CD68-specific antibody in ear of rats given tap water (LSD) or 1.0% saline (HSD), with or without additional macrophage depletion by Clod treatment, with or without additional DOCA treatment. HSD and DOCA HSD increased MPS cell count, and additional Clod treatment reversed this effect towards control level.

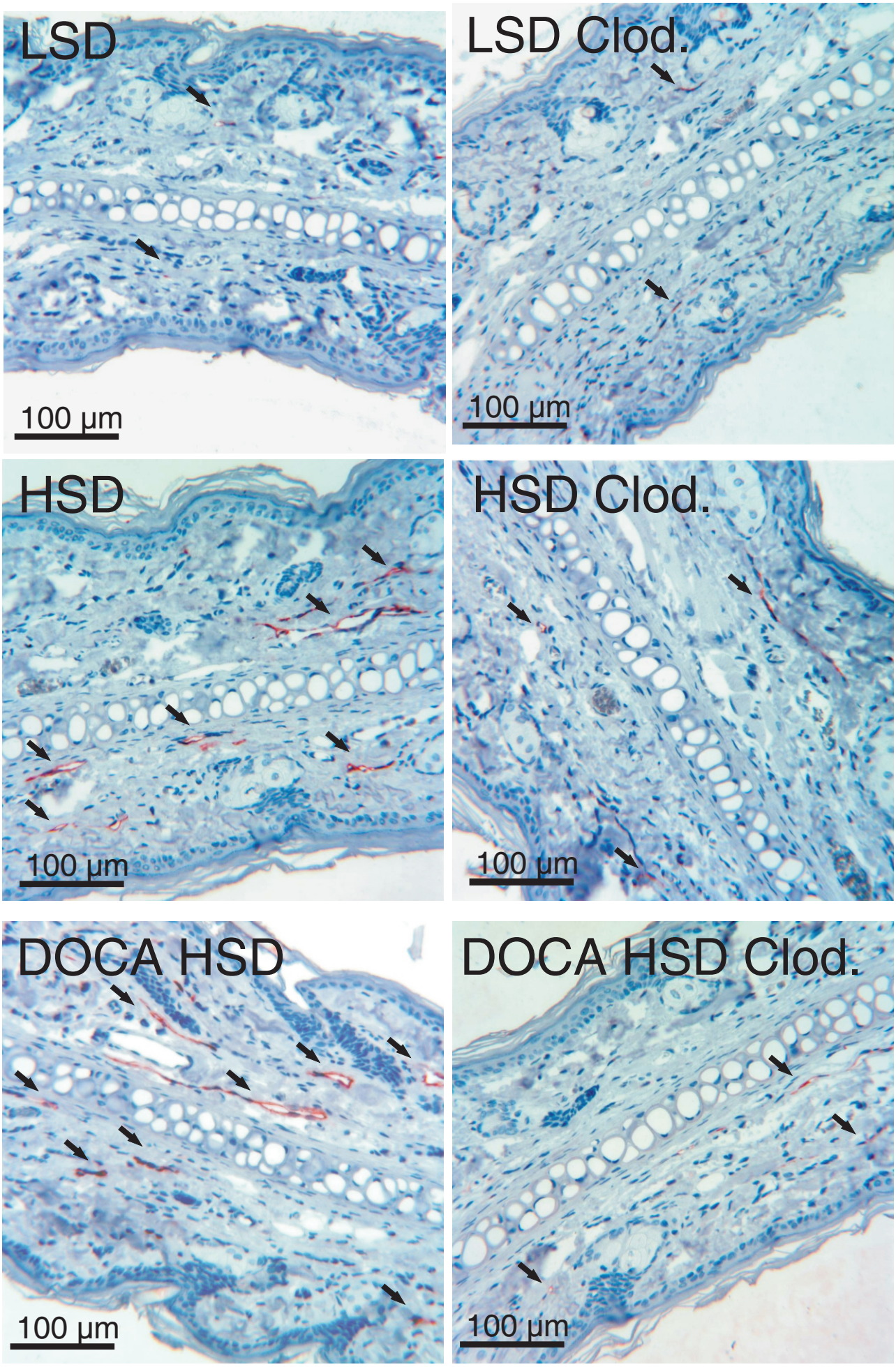

Figure S3:
Lymphatic capillaries, visualized with a podoplanin-specific antibody in ear of rats given tap water (LSD) or 1.0% saline (HSD), with or without additional macrophage depletion by Clod, with or without additional DOCA treatment. HSD and DOCA HSD increased lymph capillary count, and additional Clod treatment reversed this effect back to the control level.